COMPUTER ANIMATION AND VIRTUAL WORLDS
Comp. Anim. Virtual Worlds 2010; **21**: 55–68
Published online in Wiley InterScience
(www.interscience.wiley.com) DOI: 10.1002/cav.332

Image-based detail reconstruction of non-Lambertian surfaces

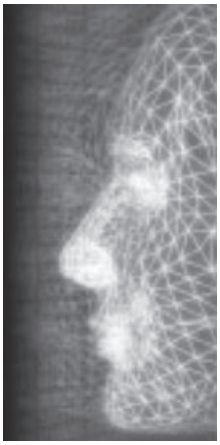

By I-Chen Lin, Wen-Hsing Chang, Yung-Sheng Lo, Jen-Yu Peng and Chan-Yu Lin*

This paper presents a novel optimization framework for estimating the static or dynamic surfaces with details. The proposed method uses dense depths from a structured-light system or sparse ones from motion capture as the initial positions, and exploits non-Lambertian reflectance models to approximate surface reflectance. Multi-stage shape-from-shading (SFS) is then applied to optimize both shape geometry and reflectance properties. Because this method uses non-Lambertian properties, it can compensate for triangulation reconstruction errors caused by view-dependent reflections. This approach can also estimate detailed undulations on textureless regions, and employs spatial-temporal constraints for reliably tracking time-varying surfaces. Experiment results demonstrate that accurate and detailed 3D surfaces can be reconstructed from images acquired by off-the-shelf devices. Copyright © 2010 John Wiley & Sons, Ltd.

Received: 19 November 2008; Revised: 5 November 2009; Accepted: 9 November 2009

KEY WORDS: image-based 3D modeling; shape-from-shading; non-Lambertian reflection ; motion capture; facial animation

Supplementary information may be found in the online version of this paper.

Introduction

Recently, the demand for digitizing static or deformable surface parameters from real objects has increased dramatically. These digitized surfaces can be manipulated as 3D models in computer graphics and animation, or they can be used as statistic data in model-based vision or other analysis techniques.

Using images from one or multiple views is a flexible and effective approach to calculating 3D positions. Passive stereo triangulation which evaluates transformation and depths from pixel correspondences, is the most popular approaches to image-based modeling. However, pixel correspondences are usually ambiguous on textureless regions where estimated depths are also unreliable.

Structured-light reconstruction which uses a camera and a projector to acquire depth images, is another popular triangulation method. In 2004, Zhang *et al*.[1] introduced an impressive system for estimating dynamic face surfaces. They exploited space-time coherence to establish a more reliable pixel-correspondence. However, they had to use high resolution devices with a fast capturing speed due to the inherent properties of coded structured-light systems. Moreover, when we scan objects with non-Lambertian properties, the projected light stripes can be distorted by specular or sub-surface scattering effects. For this reason, most experiments spread diffuse-reflected powders or paints on these kinds of objects.

On the other hand, photometric stereo methods and shape-from-shading (SFS) evaluate surface normals according to variations of image intensity. Most existing methods adopt the Lambertian reflectance model. The photometric stereo calculates the surface normals from images under different light directions but from a fixed view point. However, using photometric stereo methods for dynamic objects require expensive high-speed cameras and a light dome.[2,3] SFS methods usually illuminate the scene by a single light source and use only intensity gradients for shape recovery, avoiding ambiguity of pixel correspondence. The SFS methods are also sensitive to

*Correspondence to: I-C. Lin, Department of Computer Science, National Chiao Tung University, Taiwan.
E-mail: ichenlin@cs.nctu.edu.tw

subtle variations and are therefore adequate for acquiring detailed undulation data. Nevertheless, its sensitivity to noise may lead to serious tremble.

The goal of this paper is to enhance the detail estimation capacity of existing 3D capture devices. The proposed technique focuses on structure-light reconstruction and facial motion capture systems, and can therefore be extended to other triangulation-based systems easily. The proposed method uses the shading information to amend or enrich 3D positions by stereo triangulation. In other words, stereo triangulation evaluates absolute positions around distinct features and SFS retrieves relative undulation.

For structured-light scanning systems, bidirectional reflectance distribution function (BRDF) and bidirectional surface scattering reflectance distribution function (BSSRDF) can both correct distorted or noise-contaminated surfaces. To capture facial motion, the proposed method uses optimized shape from shading to extract time-varying wrinkles and creases, which are difficult to capture using marker tracking. Furthermore, spatial-temporal coherences are employed for more reliable tracking. Figures 1 and 2 show the proposed method applied to range scanning and motion capture systems, respectively.

Several recent studies also share the idea of combining the advantages of positioning and shading information.[4,5] Bickel *et al*.[6] enhanced facial wrinkles using reflected intensities. In contrast, the proposed iterative optimization scheme uses only one image as an input for detailed shape recovery. Moreover, since we do not need to apply additional paints or restrict the shape of details, this method can even be applied to existing capture data or recorded images.

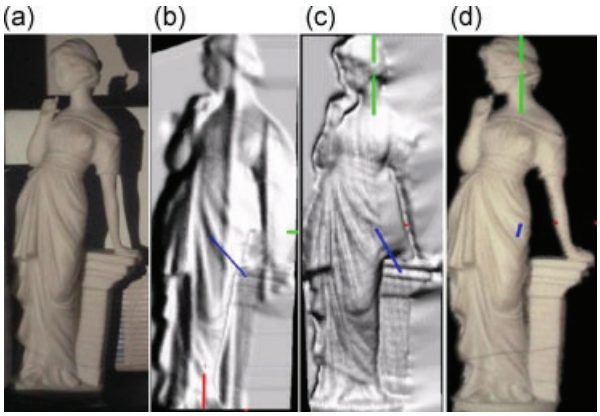

Figure 1. The proposed optimized shape-from-shading for detail refinement. (a) A captured image of the target statue. (b) The estimated surface by structured-light triangulation. The depths are distorted by input noise and stripe calibration errors. (c) The surfaces estimated by the proposed optimization. (d) The synthesized model with texture mapping.

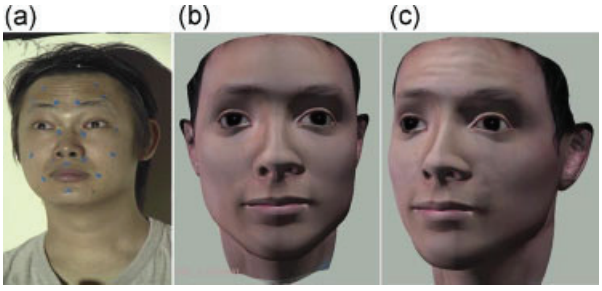

Figure 2. The proposed method for time-varying facial detailed motion. (a) A captured image of facial motion capture. (b) The retargeted face without facial details. (c) The synthesized face enhanced by the estimated wrinkles.

This paper is organized as follows. The following sections introduces most related research, followed by overview of the proposed method. The section titled "Estimating Surface Detail by SFS" proposes the progressive shape rectification method. The "SFS for sparse motion data" section applies detailed recovery to a facial motion capture system. The final section concludes this paper.

Related Work

The proposed method estimates detailed surfaces using SFS based on graphics reflection models and space-time constraints. This section provides a literature review on these topics.

Stereo triangulation has been the main approach to vision-based shape recovery for decades. However, reliable pixel correspondence remains illusive in this approach. Readers may refer to Forsyth and Ponce[7] for a detailed explanation. In 2005, Vogiatzis *et al*.[8] proposed using the visual hull as the initial volume and optimized the results by graphic-cut minimization. Their system provided a more reliable 3D surface but also suffered from the correspondence error caused by non-Lambertian reflection.

While applying triangulation for time-varying motions, conspicuous markers can alleviate this correspondence problem. Guenter *et al*.[9] proposed a dynamic face digitization system that tracked more than a hundred special markers. For time-varying facial details, they simply recorded dynamic texture.

Comp. Anim. Virtual Worlds 2010; **21**: 55–68
DOI: 10.1002/cav

Lin *et al*.[10,11] proposed capturing dense facial markers with mirror-reflected views. Even though they tracked nearly three hundred markers, they still had difficulty in reconstructing wrinkles or dimples. In 2008, Castellani *et al*.[12] proposed a robust deformable surface estimation method based on range scan data. They also accounted for spatial-temporal coherence, but excluded reflectance effect.

Anatomical models can mimic wrinkles and creases[13]. Sifakis, *et al*.[14] presented an automatic approach to determining muscle parameters based on sparse markers. However, this method cannot reproduce exact details of a performer.

On the other hand, photometric stereo and SFS methods evaluate delicate surface normals using variations of image intensity. Photometric stereo approaches usually analyze images from a fixed view point but under various lighting directions. Given accurately aligned pixels, photometric stereo methods can estimate surface normals by a simple least-square method. Empirically, more than eight images of different light directions are required to acquire reliable normals. Hertzmann and Seitz[15] proposed an example-based method in which the target surface normals were evaluated by comparing reference images of a known object. Ma *et al*.[16] proposed a novel polarized illumination method to acquire diffuse and specular normal maps. Their system is capable of estimating high-resolution detail face geometry.

In contrast, the SFS method can avoid errors caused by inaccurate pixel correspondence, and this low-cost approach requires only one image for shape recovery. Fang and Hart[17] utilized a Lambertian-reflection-based method to extract the normal map from a single texture image. This kind of approach does not require expensive devices. However, it was error-prone due to the simple Lambertian assumption and was sensitive to input noise. As a result, manual adjustments were usually required in post processing.

SFS is also difficult to apply to real data due to its intrinsic ill-condition. In interactive modeling, Zeng at al.[18] proposed a semi-automatic solution for continuous surfaces. In this approach, users assigned surface normals to specific feature points and the system then refined the surface variations of the whole face. Ahmed and Farag[19] proposed using Oren and Nayar's diffuse reflection model for more accurate SFS calculations of rough surfaces. In a later study,[20] they used perspective camera and Ward's reflection model. Since they proposed using a fast PDE solving method, their work cannot directly be applied to time-varying data with specific constraints, e.g., spatial-temporal coherence, or range constraints.

Recently, several researchers have combined stereo triangulation with shading information. Nehab *et al*.[4] proposed an efficient linear least square method that combines 3D positions with photometric normals. They assumed the objects have only Lambertian reflectance. Yu *et al*.[5] proposed a Phong-reflection-based shape recovery. They used visual hull of multiple views as the initial volume. Then, an optimization approach was employed to find the shape and reflectance parameters of static objects in the views.

Bickel *et al*.[6] proposed a multi-scale capturing system for facial motion. They first used conventional motion capture for large-scale motion. For middle-scale motions, they painted a specific color on each wrinkle and estimated parameters of the "valley-shape" wrinkle model from video.

Unlike most SFS under a Lambertian assumption, the proposed approach applies more general reflectance models. In computer graphics, the BRDF is widely used to represent the reflectance model of human faces. Assuming that human skin is composed of an oil layer, epidermis, and dermis, skin reflectance can be approximated by a specular component at the oil-air interface and a diffuse reflectance component due to subsurface scattering. For more realistic subsurface scattering, Jensen *et al*.[21,22] introduced a BSSRDF model that combines dipole diffusion approximation and single scattering computation. Such sophisticated dipole models can also be embedded in our framework.

Overview

The approach presented in this paper combines the benefits of stereo triangulation and SFS methods. Stereo-based 3D reconstruction is employed to evaluate the rough geometry, while a novel progressive SFS optimizes the detailed surfaces. We apply this framework to two applications: structured-light scanning and facial motion capture. For structured-light reconstruction, evaluated depths are set as the initial surface heights and range constraints, and the heights and reflectance parameters are refined progressively.

To capture facial motion, the proposed system first scattered the markers' 3D positions to non-marker regions by a radial-basis function (RBF). These scattered depths are then utilized as initial heights for surface optimization. In motion surface evaluation, surface heights are time-varying variables, and spatial and temporal constraints are included for more stable results. Figure 3 shows the flow chart of the proposed system.

DOI: 10.1002/cav

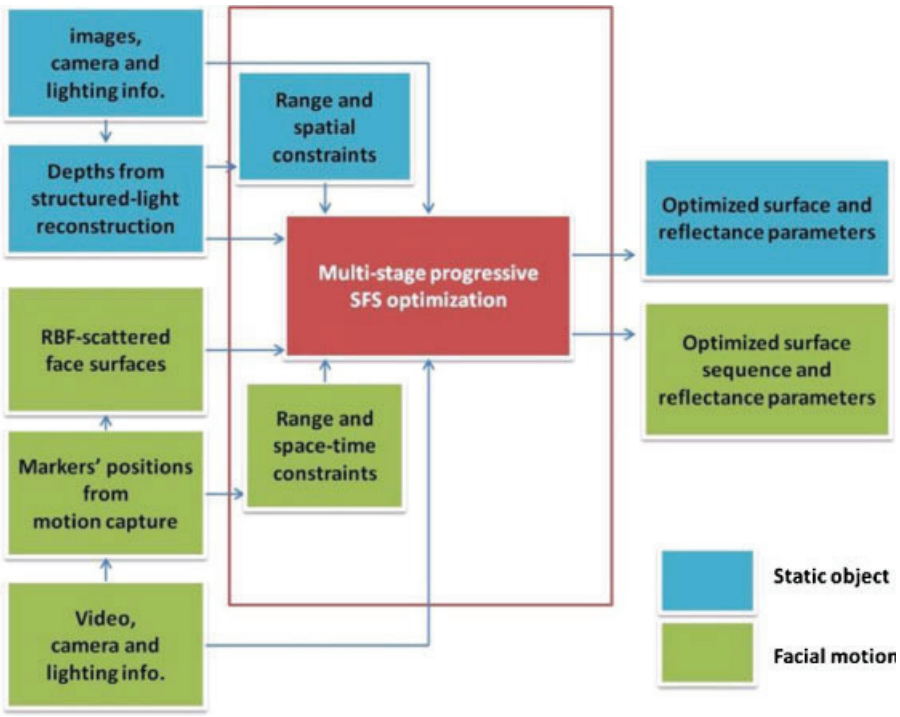

Figure 3. The flow chart of the proposed system. The optimization for static objects is in blue and that for facial motions is in green.

Estimating Surface Detail by SFS

As mentioned above, stereo reconstruction can estimate accurate depths with conspicuous features, and structured-light systems that actively project light stripes can simplify the feature identification problems in textureless regions. We set up one video camera and one digital projector to form a structured light system. The projected light stripes are calibrated by a method proposed by Huynh.[23] Figure 4 shows the progress of scanning a marble statue.

Objective Functions of SFS

After acquiring the initial positions, we utilize shape from shading to refine the surface according to shaded surface intensity. We adopt an optimization method that minimizes the difference between the captured image I and the synthesized image S. The objective function O_{static} becomes

$$O_{\text{static}} = (S - I)^2 \tag{1}$$

To decrease the degrees of freedom (DOF) of an objective function, without loss of generality, we represent the 3D data in terms of a height map. These heights can be easily transformed to normals from the gradients of neighbor z values. Hence, only the z (height) values of each aligned pixel (vertex) are evaluated. The shape parameters Z are therefore defined as

$$Z = (z_1, z_2, \ldots, z_p, \ldots, z_{n_p})$$

where n_p is the number of pixels(vertices).

We choose the Phong model as the analytic reflection model, but other BRDF models can also be applied. The Phong model is widely used in computer graphics and its differentiation of parameters is relatively straightforward. Given a light source L with direction N_L and the surface normal N_p, the reflection intensity on vertex p related to normal can be written as

$$S_p(N_p, K_d, K_s) = I_d \cdot k_d(N_L \cdot N_p) + I_s \cdot k_s(e \cdot r)^{\alpha} \tag{2}$$

where k_d and k_s are the diffuse and specular coefficients and α is the Phong exponent term. The vector e denotes the view direction and r is the reflection vector with respect to N_L and N_p.

DOI: 10.1002/cav

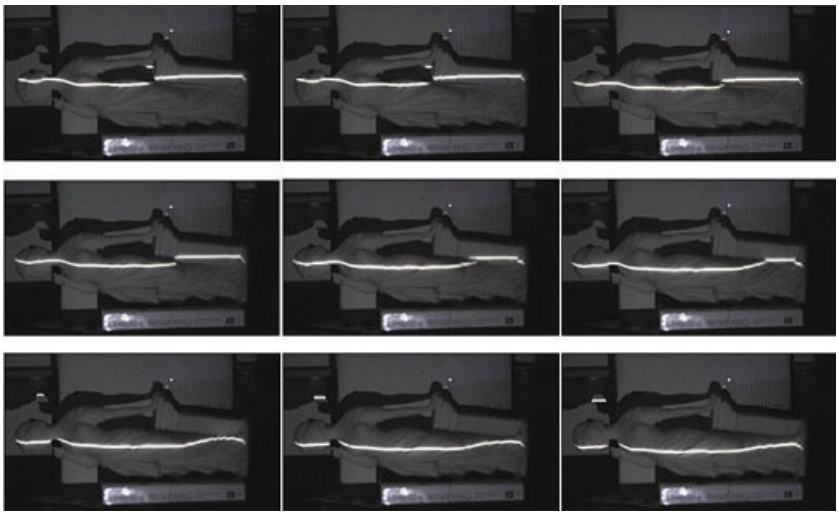

Figure 4. Scanning a marble statue by a structured-light system.

Assume that the reflectance parameter of a subject's face, $R = (k_d, k, \alpha)$, is uniform in a region. Equation (1) then becomes

$$O(Z, R) = \sum_{p=1}^{n_p} (S_p - I_p)^2 \tag{3}$$

In other words, our goal is to find the best surface sequence Z^* and reflectance parameter R^* that minimize the objective function. Instead of BRDF models, the BSSRDF model proposed by Jensen *et al*.[21] can also be applied as

$$S_p(N_p, \sigma_s, \sigma_a) = \frac{\acute{\alpha} z_r (1 + \sigma_{\mathrm{tr}} d_{r,i}) e^{-\sigma_{\mathrm{tr}} d_r}}{4\pi d_r^3} - \frac{\acute{\alpha} z_v (1 + \sigma_{\mathrm{tr}} d_{v,i}) e^{-\sigma_{\mathrm{tr}} d_v}}{4\pi d_v^3} \tag{4}$$

where $\sigma_{\mathrm{tr}} = \sqrt{3\sigma_a \sigma_t'}$ is the effective transport coefficient, $\sigma_t' = \sigma_a + \sigma_s'$ is the reduced extinction coefficient, $\alpha' = \sigma_s'/\sigma_t'$ is the reduced albedo, and σ_a and σ_s' are the absorption and reduced scattering coefficients. $z_r = 1/\sigma_t'$ and $z_v = (1 + 4A/3)/\sigma_t'$ are the z-coordinates of the positive and negative sources relative to the surface at $z = 0$. $r = \|x_o - x_i\|_2$ and $d_r = \sqrt{r^2 + z_r^2}$ and $d_v = \sqrt{r^2 + z_v^2}$ are the distances to the sources from a given point on the surface of the object. A is defined as

$$A = \frac{(1 + F_{\mathrm{dr}})}{(1 - F_{\mathrm{dr}})}$$

where F_{dr} is the diffuse Fresnel reflectance. Readers can refer to [21] for a detailed explanation.

Multiple-Stage Optimization

Experiment results show that the estimated heights were highly sensitive to noise when applying direct SFS methods.[17] When we used the heights from structured-light scanning as initial values and applied modified conjugate-gradient methods, these variables were easily trapped into local minima in early stages, producing undesired trembling effects. For more stable estimation, we propose using a multi-stage optimization scheme.

Our objective function has two sets of parameters: the shape parameter Z and reflectance parameter R. If we simultaneously estimate these two parameters into a single stage, we need a proper scale between these two kinds of parameters for balanced influences. To avoid bias, we optimize these two sets of parameters separately.

Experiment results also show that when directly applied all BRDF parameters in optimization, the specular components dominated the objective function, trapping the process in a local minimum. On the other hand, the reflections of human skin or marble statues are mainly contributed by diffuse components. Hence, we introduce an intermediate stage, diffuse-shape optimization in which the shape Z and diffuse parameter *R-diffuse* (kd) are iteratively optimized. After this stage, BRDF-shape optimization is performed for all diffuse and specular parameters. Figure 5 shows the flow chart

DOI: 10.1002/cav

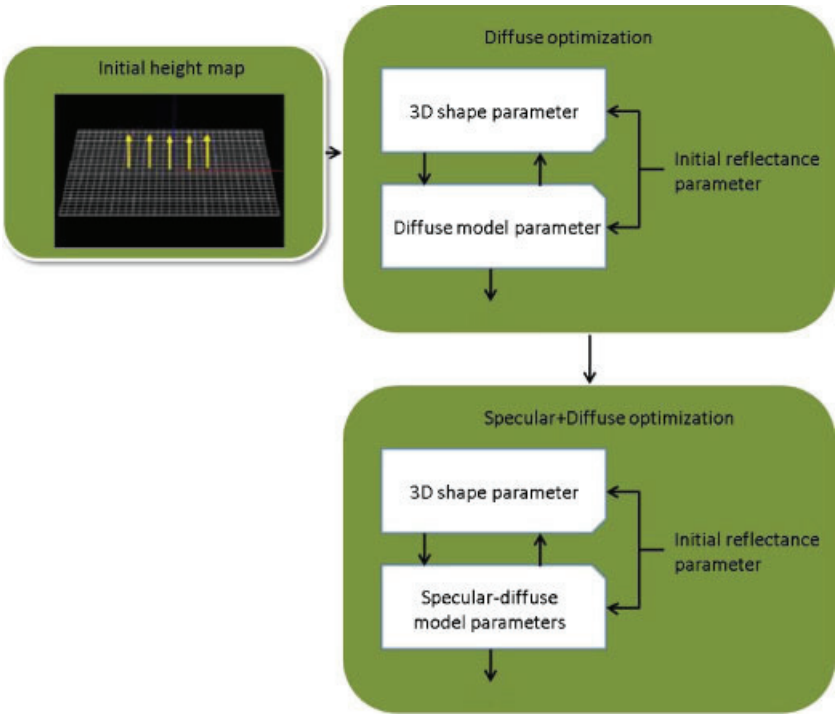

Figure 5. The flow chart of multi-stage optimization.

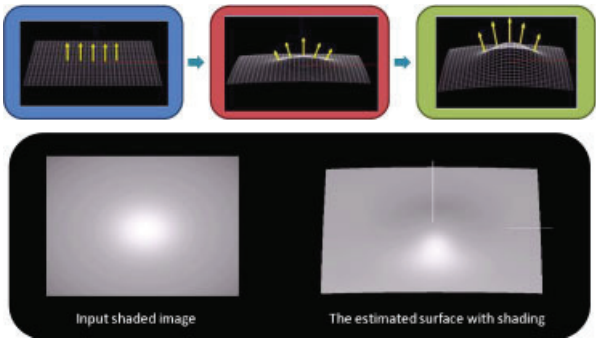

Figure 6. A conceptual diagram of progressive surface estimation with a height map.

of the multi-stage optimization. Figure 6 shows a conceptual diagram of optimized SFS.

Spatial Coherence and Range Constraints

Since our targets, e.g., faces, are mostly continuous surfaces, the motion of a vertex p has a high spatial coherence with its neighbors. Therefore, we use spatial coherence constraints to alleviate the inherent noise sensitivity in the SFS approach.

$$\mathrm{CS}_p = k_{\mathrm{CS}} \left(z_p - \sum_j \frac{1}{w_j} z_j \right)^2, \quad \text{for } j \in \mathrm{Neighbor(tp)} \tag{5}$$

, where Neighbor(p) denotes the 8-neighbor pixel set, w_j is an adaptive weight, and k_{CS} is the weight for spatial constraints. After transforming the corresponding height-map block to the frequency domain, an area will be more influenced by its neighbors if it is dominated by low-frequency components beyond a certain threshold. Figure 7 shows the influence of spatial constraints.

Moreover, since the scanned surfaces are near the exact positions and SFS is aimed at adjusting relative undulation, range constraints CR can be used to keep the heights

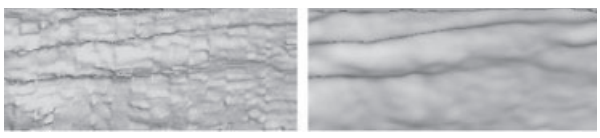

Figure 7. The influence of spatial coherence constraints. (left) the optimized surface without spatial constraints. (right) the result with spatial constraints.

Comp. Anim. Virtual Worlds 2010; **21**: 55–68
DOI: 10.1002/cav

near the original scans.

$$\mathrm{CR}_p = -k_{\mathrm{CR}} e^{-(z_p - z'_p)^2} \tag{6}$$

where k_{CR} is the weight for range constraints and z'_p is the estimated height of pixel p by triangulation.

Shape-from-Shading for Sparse Motion Data

The space-time study of Zhang *et al.*[1] extends a stereo structured-light system to facial motion capture. Nevertheless, structured-light reconstruction acquires multiple stripe sets for one surface, and therefore requires higher capture rate for time-varying surfaces.

Instead, the proposed study tracks facial details by extending widely used motion capture techniques. Since motion capture techniques only track markers' 3D trajectories, we first have to reconstruct the rough initial surfaces according to the sparse markers' 3D positions.

Initial Surfaces from Motion Capture

To evaluate time-varying primitive 3D face surfaces, we adopt a model-based approach. First, the 3D positions of markers in the first frame are estimated by stereo triangulation. We then characterize a generic face model by feature-point fitting, which is similar to the deformation method described below.

Assume that the expression at the initial frame is neutral. For each of the following frames, track the markers and deform the characterized model according to the markers' 3D positions. The deformation method employed in this study is radial-basis-function-based (RBF-based) data scattering.

Consider a set of corresponding pairs $\{q_i,\ q(t)_i\}$ between the neutral face and an expressional face at time t, where q_i is the 3D position of the marker i on the neutral face, and $q(t)_i$ is the position of the marker on an expressional face at time t. We define the motion (displacement) of each marker as $u(t)_i = q(t)_i - q_i$, and use scattering function $F(t, q)$ to estimate the displacement of a non-feature point. The scattering function at time t is then

$$F(t, q) = \sum_i c(t)_i \varphi(\|q - q_i\|) + A(t)q + B(t) \tag{7}$$

where $\varphi(r) = e^{-r/32}$ is a radial basis function. $c(t)_i$ are weighted coefficients, and $A(t)$, $B(t)$ are affine terms. The coefficients $c(t)_i$, $A(t)$, and $B(t)$ can easily be solved by linear equations with the following constraints:

$$u(t)_i = F(t, q_i), \sum_i c(t)_i = 0, \sum_i c(t)_i q_i = 0$$

Figure 8 shows an example of a personalized face surface driven by captured markers.

Spatial-Temporal Coherence

When applying our optimized SFS to each frame individually, we found that there were still flickers caused by input noise. According to the biomechanical properties of facial muscles and tissues, the surface of a human face should gradually transfer between expressions. Hence, temporal coherence can further improve stability.

The first step is to extend our shape representation Z to a time-varying form:

$$Z_t = (z_{t1}, z_{t2}, \ldots, z_{tp}, \ldots, z_{t(n_p)})$$

where t is an index of time (or frame).

Applying optimization to the entire image sequence is extremely time-consuming. For computational efficiency, we only apply our optimization to a small window of frames at a time (7 frames in this case). A pseudo-optimal surface sequence can be acquired by sweeping the windows from the start to the end and combining the individual results. This approach significantly decreases the degrees of freedom and dramatically reduces processing time.

The temporal constraint then becomes

$$\mathrm{CT}_{tp} = k_{\mathrm{CT}} \left(z_{\mathrm{tp}} - \sum_i \frac{1}{w_i} z_{(t+1)p} \right)^2, \text{ where } \quad i = [-3, 3] \tag{8}$$

Therefore, including time-varying variables and spatial-temporal coherence and range constraints, our objective function becomes

$$O = \sum_{t=1}^{n_t} \sum_{p=1}^{n_p} \left[(S_{\mathrm{tp}} - I_{\mathrm{tp}})^2 + \mathrm{CS}_{\mathrm{tp}} + \mathrm{CT}_{\mathrm{tp}} + \mathrm{CR}_{\mathrm{tp}} \right]) \tag{9}$$

where S_{tp}, I_{tp}, $\mathrm{CS}_{\mathrm{tp}}$, and $\mathrm{CR}_{\mathrm{tp}}$ are the extenstions of S_p, I_p, CS_p and CR_p with time indices.

DOI: 10.1002/cav

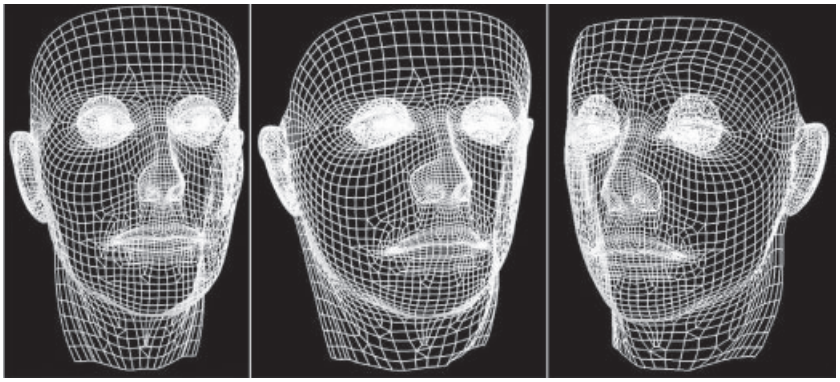

Figure 8. Deformation of a generic model for personalization and facial expression. (left) the generic model; (middle) the personalized neutral face; (right) eyebrow raising according to markers' positions.

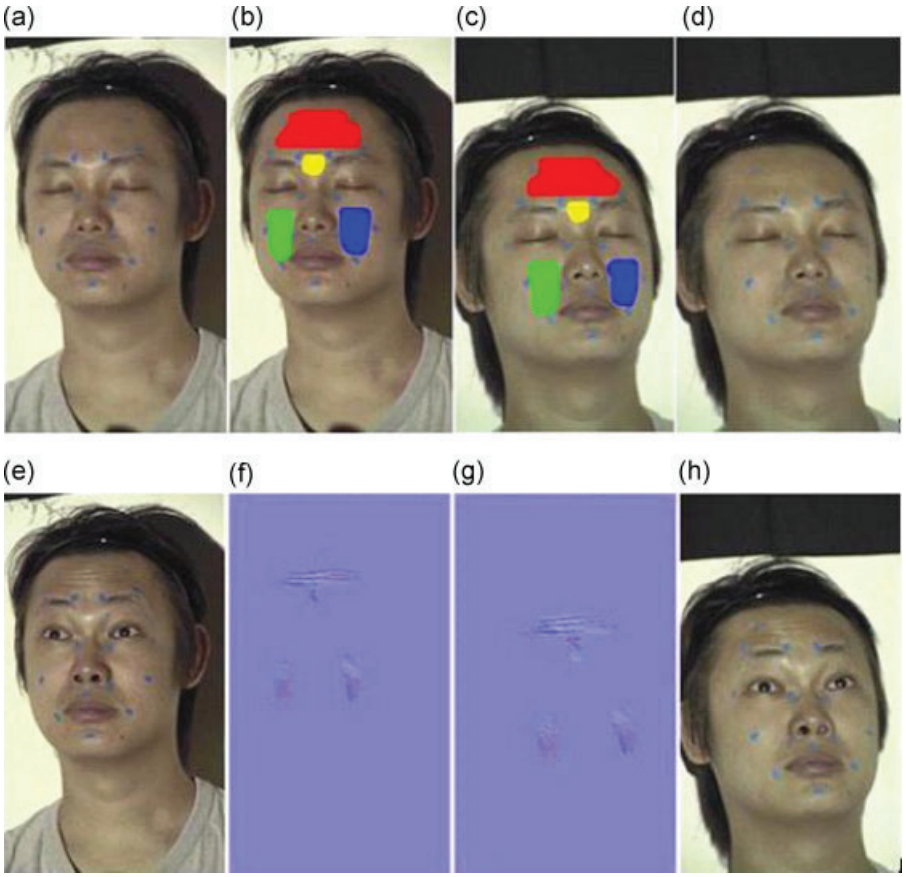

Figure 9. The captured two-view image and extracted detailed surfaces. (a)(d) are the right and left views of the neutral face; (b)(c) are the user-assigned regions for evaluation; (e)(h) are the right and left views of an expressional face; (f)(g) are the estimated detailed surfaces of (e) and (h).

Comp. Anim. Virtual Worlds 2010; **21**: 55–68
DOI: 10.1002/cav

Experiments and Results

This section describes and discusses our experiments and error analysis, and presents results of static objects and facial motions.

Experiments

The proposed system uses one video camera and one projector for structured-light reconstruction. To simplify the optimization, all our experiments were performed under an illumination-controlled environment. A calibrated spotlight served as a single directional light source. The high-definition video(HDV) cameras used in this setup had a resolution of 1280*720 pixels and a 30 frames-per-second capture rate.

For facial surfaces, two synchronized video cameras were applied to track marker motions. We pasted 25–30 markers on subjects' faces, being careful not to place markers on regions with wrinkles or creases. Three subjects, one female and two males, were requested to give various facial expressions. Since the proposed technique is designed to enhance delicate variations in motion capture, users can assign regions for detail estimation. In our experiments, we preferred areas with more creases, such as the forehead, glabella, left, and right cheeks. Figure 9 shows the captured neutral image and the user-assigned regions by a brush-based interface.

Moreover, since our goal is to extend the usage of existing devices, the proposed system can use the images from structured-light or motion capture to optimize SFS directly. In motion capture, we used two views, and therefore two height maps were acquired. Given two synchronized height maps and feature points, the view morphing technique[24] was applied to warp the two side views into a single front one. Then, we weighted-blended the two sets of view data according to the view angles.

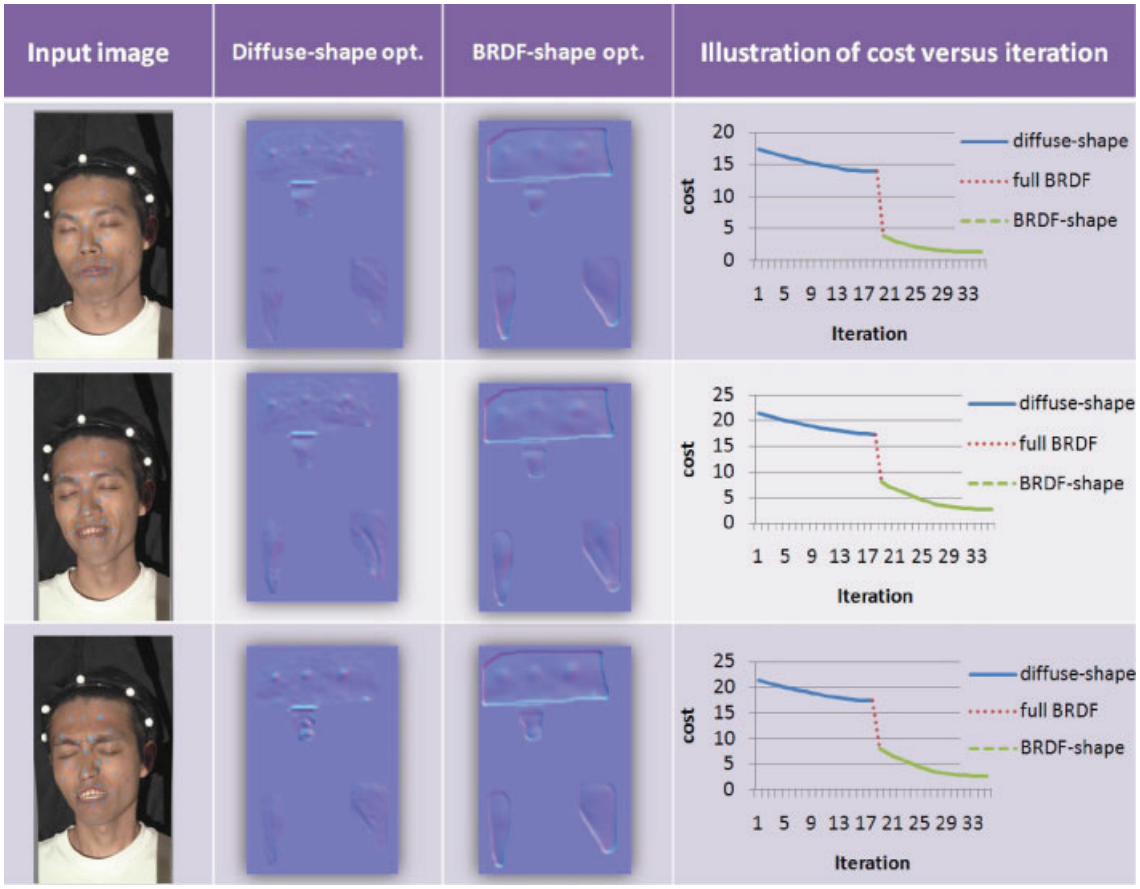

Figure 10. Iterative recovery of a facial surface sequence. The leftmost column shows the input image; the middle two columns demonstrate the estimated normal maps at diffuse-shape and BRDF-shape stages. The rightmost column shows the cost versus iteration time.

Comp. Anim. Virtual Worlds 2010; **21**: 55–68
DOI: 10.1002/cav

Data that are closer to their original view get a higher ratio.

The proposed system adopts a conjugate-gradient-based method, called the Broydon-Fletcger-Goldfarb -Shanno (BFGS) method, for non-linear function minimization. At each iteration, we first estimated the approximate step direction, and the golden section search was further utilized to find the optimal step size. In facial motion estimation, where four mid-small size regions are evaluated, the performance of our optimization was around 120–200 seconds per frame on a PC with a 3.2 GHz CPU; for scanned objects, the minimization took nearly one hour per view. Since the current system only uses single-threaded programming, the computation time can be further improved with multi-threaded programming.

Figure 10 demonstrates the progress of cost *versus* iteration time for three exemplary frames in a facial motion

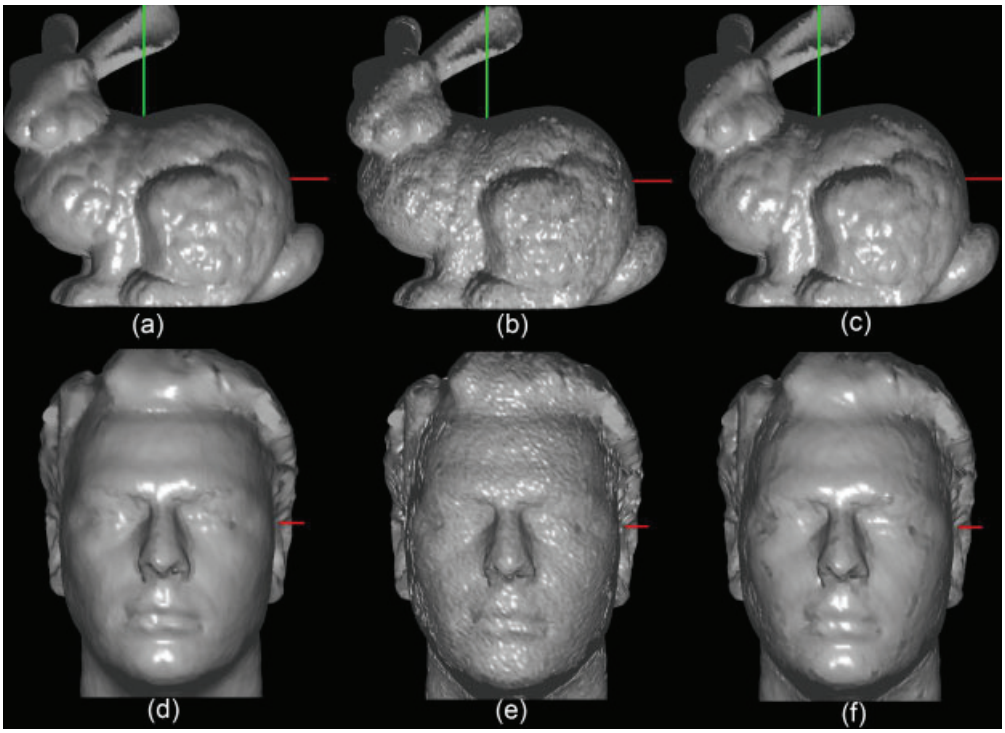

Figure 11. Error analysis of SFS correction with Phong- reflection objects by simulation. (a) The ground-truth bunny; (b) the noise-contaminated bunny; (c) the SFS-corrected bunny; (d) the ground-truth head; (e) the noise-contaminated head; (f) the SFS-corrected head.

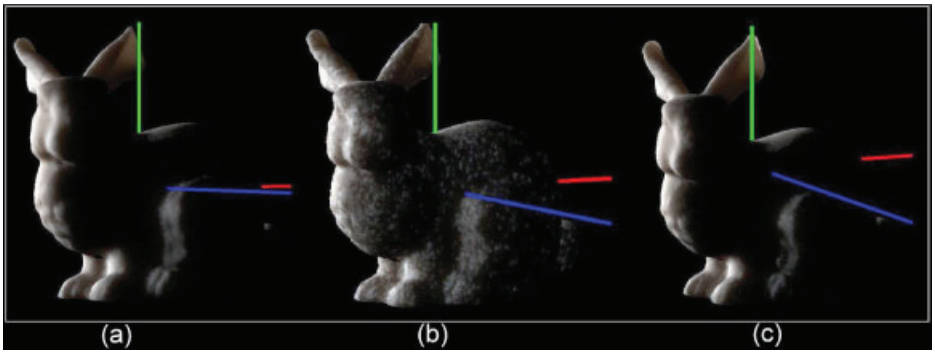

Figure 12. Error analysis of SFS correction with BSSRDF-reflection objects (with known BSSRDF- reflection parameters). (a)The ground-truth bunny; (b) the noise-contaminated bunny; (c) the SFS-corrected bunny.

Comp. Anim. Virtual Worlds 2010; **21**: 55–68
DOI: 10.1002/cav

sequence. The cost here is the error between the input image and synthesized image. In our evaluation, we normalized the intensity of a pixel to range [0,1]. The cost gradually decreased during the diffuse-shape optimization. When specular parameters were included in reflectance optimization, the cost dropped significantly. BRDF-shape optimization further improved the shape and evaluated BRDF parameters.

Error Analysis

We evaluated the performance of the proposed detail estimation method by computer simulation. Two virtual models, "bunny" and "human head", were selected as targets. We assumed the "heights" (max y - min y values) of these models were 200 mm, and applied random noises of maximum 2 mm to their vertices. Given the noise-contaminated models and the shaded images of ground-truth models, we applied our multi-stage SFS for surface rectification. Figure 11 shows the experiments based on Phong reflection model. In this case, the per-vertex errors of the human head were reduced from 0.634715 to 0.236203 mm, while the bunny's were reduced from 1.035466 to 0.991826 mm. Even though the error improvement of the high curvature "bunny" model is less obvious, the refined model is visually more appealing and closer to the ground-truth due to our appearance-based algorithm.

We also performed this analysis to BSSRDF-reflection objects. Nevertheless, we found that the optimization of BSSRDF parameters diverged easily and required precise initial guesses. Therefore, in BSSRDF experiments,

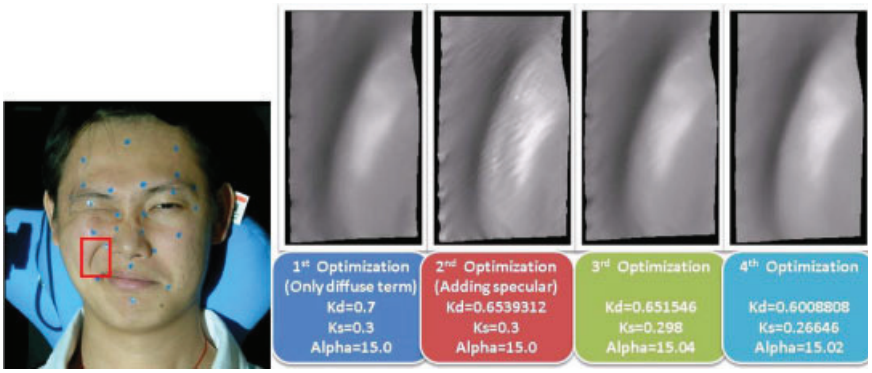

Figure 13. The progressive surface refinement for a captured wrinkle image.

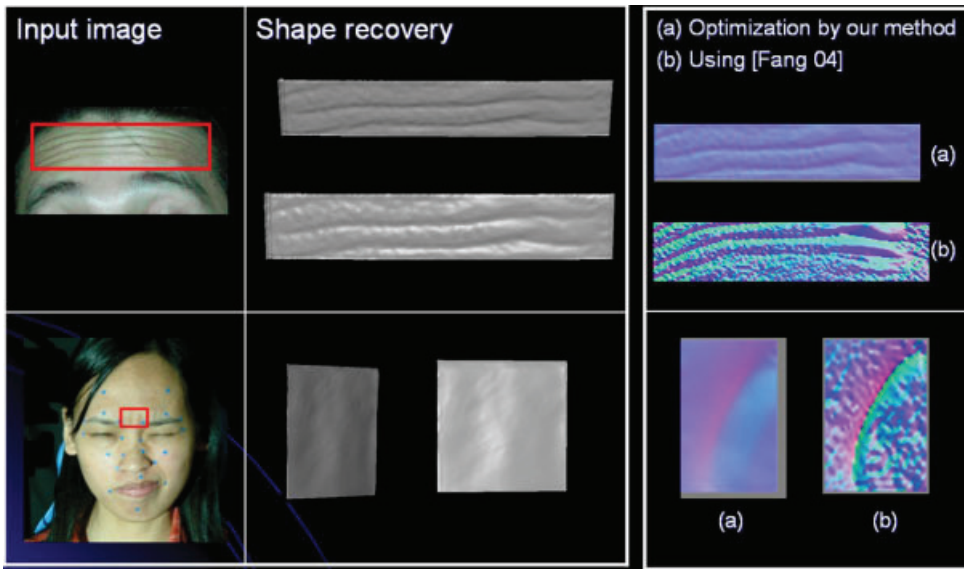

Figure 14. Comparison of the proposed space-time SFS method and a Lambertian- based direct SFS method.

Comp. Anim. Virtual Worlds 2010; **21**: 55–68
DOI: 10.1002/cav

we only performed height optimization and the BSSRDF reflectance parameters were assumed to be known. Figure 12 shows that random noises of maximum 5 mm were embedded in the bunny model. After our position optimization with BSSRDF reflection, the average per-vertex error was reduced from 3.554 to 0.031 mm.

Figure 13 shows the progress of optimization in terms of stages. In the first stage, the diffuse term is optimzed to obtain a more accurate shape. The second stage includes specular terms. The estimated surfaces gradually approached the input image sequence. Figure 14 also compares our space-time SFS with a direct Lambertian-based method.[17] Our method provides more accurate surface and suppresses noise.

Synthesis of Faces

We derived a characterized neutral face according to motion capture data. Our 3D head model contained 6078 vertices and 6315 polygons. For deformation, we applied RBF-based data scattering to each segment and gradually blended the boundaries. To enhance details with estimated height maps, the target polygons were first subdivided and per-pixel normal mapping was then applied. Figure 15 depicts the face with detail wrinkles. The synthesized results can be further improved with relief textures and realistic face rendering. Besides, our acquired motion can be also employed for detailed expression synthesis, e.g., the work of Golovinskiy *et al*.[25].

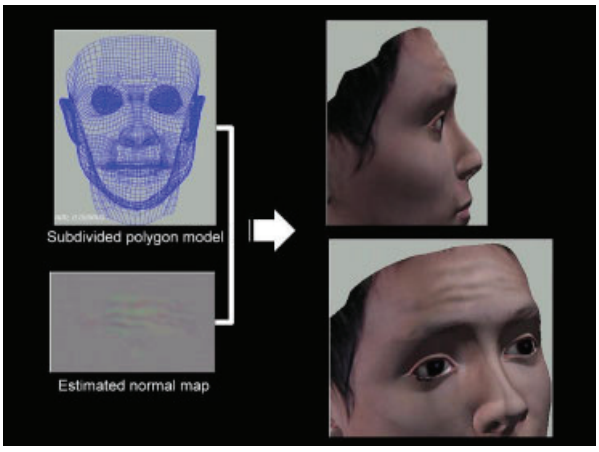

Figure 15. Facial details synthesized by subdivision and normal mapping.

Discussion and Conclusion

The goal of this paper is to estimate non-Lambertian-reflected surface details by off-the-shelf devices. The proposed approach combines the advantages of stereo triangulation and SFS for static scanning and facial motion. The depths estimated from triangulation are employed as initial surfaces and range constraints for optimization. The system then minimizes the error between the input and synthesized images.

To tackle the optimization problem with considerable reflectance and time-varying shape parameters, we propose an iterative scheme with multiple stages, in which diffuse parameters, diffuse-specular parameters, and the heights of surfaces are improved sequentially. Spatial and temporal coherence constraints are also included for more reliable estimation. Simulations and experimental results demonstrate the effectiveness of the proposed method.

Compared with the related articles,[5,6] where impressive shapes were evaluated from multiple static views or specific groove models, the proposed method is more versatile for various details with dense or sparse initial depths. We neither assume the shape of details nor spread powder or paint for diffuse reflection. If the illumination is controlled, the proposed method can even be applied to existing scanning or motion capture video.

The proposed method can be adapted to various non-Lambertian reflection models. To our best knowledge, the proposed system could be the first paper applying the BSSRDF reflection[21] to shape from shading. Experiment results show that a precise evaluation of reflectance parameters significantly improve the shape recovery, but optimizing reflection parameters is easily trapped in local minima, especially for complex subsurface scattering. Therefore, we can only perform position optimization in that situation. For real BSSRDF surface estimation, more intensive computations with global or heuristic optimization, e.g., simulated annealing, can alleviate this situation. The current approach assumes that reflection properties are uniform at each user-defined region. We plan to include automatic segmentation of the surface reflection in the future.

ACKNOWLEDGEMENTS

The authors would like to thank CAIG lab members, especially Chao-Chih Lin and Zhi-Han Yen, for their assistance in experiment. This work was supported in part by National Science Council, Taiwan with grant number 95-2221-E-009 -164 -MY3.

DOI: 10.1002/cav

References

1. Zhang L, Snavely N, Curless B, Seitz SM. Spacetime faces: high resolution capture for modeling and animation. *Proceedings of ACM SIGGRAPH*, 2004; 548–558.
2. Wenger A, Gardner A, Tchou C, Unger J, Hawkins T, Debevec P. Performance relighting and reflectance transformation with time-multiplexed illumination. *ACM Transaction Graphics* 2005; **24**(3): 756–764.
3. Weyrich T, Matusik W, Pfister H, *et al*. Analysis of human faces using a measurement-based skin reflectance model. *ACM Transaction Graphics* 2006; **25**(3): 1013–1024.
4. Nehab D, Rusinkiewicz S, Davis J, Ramamoorthi R. Efficiently combining positions and normals for precise 3d geometry. *Proceedings of ACM SIGGRAPH*, 2005; 536–543.
5. Yu T, Xu N, Ahuja N. Recovering shape and reflectance model of non-lambertian objects from multiple views. *Proceedings of IEEE CVPR*, 2004; 226–233.
6. Bickel B, Botsch M, Angst R, *et al*. Multi-scale capture of facial geometry and motion. *ACM Transaction Graphics* 2007; **26**(3): 33.1–33.10.
7. Forsyth DA, Ponce J. *Computer Vision: A Modern Approach*. Prentice Hall, 2002.
8. Vogiatzis G, Torr PHS, Cipolla R. Multi-view stereo via volumetric graph-cuts. *Proceedings of IEEE Computer Vision and Pattern Recognition*, 2: 391–398, 2005.
9. Guenter B, Grimm C, Wood D, Malvar H, Pighin F. Making faces. *Proceedings of ACM SIGGRAPH*, 1998; 55–66.
10. Lin I-C, Yeh J-S, Ouhyoung M. Extracting 3d facial animation parameters from multiview video clips. *IEEE Computer Graphics and Applications* 2002; **22**(6): 72–80.
11. Lin I-C, Ouhyoung M. Automatic and efficient capture of dense 3d facial motion parameters from video. *The Visual Computer* 2005; **12**(6): 355–372.
12. Castellani U, Gay-Bellile V, Bartoli A. Robust deformation capture from temporal range data for surface rendering. *Computer Animation and Virtual Worlds* 2008; **19**: 591–603.
13. Magnenat-Thalmann N, Kalra P, Luc Leveque J, Bazin R, Batisse D, Querleux B. A computational skin model: fold and wrinkle formation. *IEEE Transactions Information Technology in Biomedicine* 2002; **6**(4): 317–323.
14. Sifakis E, Neverov I, Fedkiw R. Automatic determination of facial muscle activations from sparse motion capture marker data. *ACM Transactions Graphics* 2005; **24**(3): 417–425.
15. Hertzmann A, Seitz SM. Example-based photometric stereo: shape reconstruction with general, varying brdfs. *IEEE Transactions Pattern Analysis and Machine Intelligence* 2005; **27**(8): 1254–1264.
16. Ma W, Hawkins T, Peers P, Chabert C, Weiss M, Debevec P. Rapid acquisition of specular and diffuse normal maps from polarized spherical gradient illumination. *Eurographics Symposium on Rendering*, 2007.
17. Fang H, Hart JC. Textureshop: texture synthesis as a photograph editing tool. *ACM Transaction Graphics* 2004; **23**(3): 354–359.
18. Zeng G, Matsushita Y, Quan L, Shum HY. Interactive shape from shading. *Proceedings of IEEE Conference Computer Vision and Pattern Recognition*, 1: 2005; 343–350.
19. Ahmed AH, Farag AA. A new formulation for shape from shading for non-lambertian surfaces. *Proceedings of IEEE Conference Computer Vision and Pattern Recognition*, 2: 2006; 1817–1824.
20. Ahmed AH, Farag AA. Shape from shading under various imaging conditions. *Proceedings of IEEE Conference Computer Vision and Pattern Recognition*, 2007; X1–X8.
21. Jensen HW, Marschner S, Levoy M, Hanrahan P. A practical model for subsurface light transport. *Proceedings of ACM SIGGRAPH*, 2001; 511–518.
22. Donner C, Jensen HW. Light diffusion in multilayered translucent materials. *ACM Transactions Graphics* 2005; **24**(3): 1032–1039.
23. Huynh D. Calibration of a structured light system: a projective approach. *Proceedings IEEE CVPR*, 1997; 225–230.
24. Seitz SM, Dyer CR. View morphing. *Proceedings of ACM SIGGRAPH*, 1996; 21–30.
25. Golovinskiy A, Matusik W, Pfister H, Rusinkiewicz S, Funkhouser T. A statistical model for synthesis of detailed facial geometry. *ACM Transactions Graphics* 2006; **25**(3): 1025–1034.

Authors' biographies:

I-Chen Lin is an assistant professor in the Department of Computer Science, National Chiao Tung University, Taiwan. His research interests include computer graphics and animation, especially in facial and character animation, motion capture, and image-based modeling. He received a B.S. and a Ph.D. in computer science from National Taiwan University in 1998 and 2003, respectively. He is a member of ACM SIGGRAPH and IEEE.

Wen-Hsing Chang received a M.S. degree from Institute of Computer and Information Science, National Chiao Tung University, Taiwan, in 2007. He received a B.S. in computer science from Soochow University in 2005. His research interests include computer graphics and vision, especially in 3D object modeling.

Comp. Anim. Virtual Worlds 2010; **21**: 55–68
DOI: 10.1002/cav

Yung-Sheng Lo received a M.S. degree from Institute of Computer and Information Science, National Chiao Tung University, Taiwan, in 2007. He received a B.S in computer science from Tamkang University, in 2005. His research interests include computer graphics and animation, especially in facial animation and motion capture.

Jen-Yu Peng is a PhD student in the Department of Computer Science, National Chiao Tung University, Taiwan. He received a B.S and a M.S in computer science from National Don Hwa University. His research interests include computer animation and game programming.

Chan-Yu Lin received a M.S. degree from the Institute of Multimedia Engineering, National Chiao Tung University, Taiwan, in 2009. He received a B.S. degree from National Sun Yat-sen University in 2007. His research interests include computer graphics and vision, especially in texture synthesis and 3D object modeling.

DOI: 10.1002/cav